PREDICTION OF THE NUGGET SIZE IN RESISTANCE SPOT WELDING WITH A COMBINATION OF A FINITE-ELEMENT ANALYSIS AND AN ARTIFICIAL NEURAL NETWORK

NAPOVEDOVANJE PODROČJA PRETALITVE PRI UPOROVNEM VARJENJU S KOMBINACIJO ANALIZE KONČNIH ELEMENTOV IN UMETNIH NEVRONSKIH MREŽ

Davood Afshari[1], Mohammad Sedighi[1], Mohammad Reza Karimi[1], Zuheir Barsoum[2]

[1]School of Mechanical Engineering, Iran University of Science and Technology, Tehran, Iran
[2]Department of Aeronautical and Vehicles Engineering, KTH – Royal Institute of Technology, Stockholm, Sweden
sedighi@iust.ac.ir

The goal of this investigation is to predict the nugget size for a resistance spot weld of thick aluminum 6061-T6 sheets 2 mm. The quality and strength of spot welds determine the integrity of the structure, which depends thoroughly on the nugget size. In this study, the finite-element method and artificial neural network were used to predict the nugget size. Different spot welding parameters such as the welding current and the welding time were selected to be used for a coupled, thermal-electrical-structural finite-element model. In order to validate the numerical results a series of experiments were carried out and the nugget sizes were measured. The results obtained with the finite-element analysis were used to build up a back-propagation, artificial-neural-network model for the nugget-size prediction. The results revealed that a combination of these two developed models can accurately and rapidly predict the nugget size for a resistance spot weld.

Keywords: resistance spot weld, nugget size, finite-element analysis, artificial neural network, aluminum alloys

Cilj te preiskave je napovedati velikost področja pretalitve pri uporovno zvarjeni aluminijasti pločevini 6061-T6, debeli 2 mm. Kvaliteta in trdnost točkastega zvara določata celovitost konstrukcije, kar je odvisno predvsem od velikosti področja pretalitve. V tej študiji sta bili za napovedovanje velikosti področja pretalitve uporabljeni metoda končnih elementov in umetna nevronska mreža. Izbrani so bili različni parametri varjenja, kot sta varilni tok in čas varjenja, za skupni termično-električno-strukturni model končnih elementov. Za oceno numeričnih rezultatov je bilo izvršenih več preizkusov in izmerjena je bila velikost področja pretalitve. Rezultati, dobljeni iz analize končnih elementov, so bili uporabljeni za gradnjo modela umetne nevronske mreže za napovedovanje velikosti področja pretalitve. Rezultati so odkrili, da kombinacija teh dveh razvitih modelov lahko zanesljivo in hitro napove velikost področja pretalitve pri uporovnem točkastem zvaru.

Ključne besede: uporovni točkasti zvar, velikost področja pretalitve, analiza končnih elementov, umetna nevronska mreža, zlitine aluminija

1 INTRODUCTION

Resistance spot welding (RSW) is one of the most important and well-known methods of sheet joining in various industries, especially in the automobile and aerospace industries. The process is ideal for joining low-carbon steel, stainless steel, nickel, and aluminum or titanium alloy components with various thicknesses and it is, thus, used extensively. Although each material has its own particular place and special importance, today, aluminum alloys are the most widely used materials after steel. Though spot welding of aluminum alloys is more difficult than spot welding of steels because of their narrow plastic rang, low bulk resistance and greater thermal conductivity, aluminum alloys are still used for the bodies and chassis of many components due to their lightweight and relatively high strength resulting in a reduction of a vehicle structural weight, fuel consumption and exhaust emissions.[1,2]

Typically, a modern automotive vehicle contains 2000–5000 spot welds and the joint quality and performance can dramatically alter the structural performance of vehicles, having a critical role in durability and safety design of vehicles.[3] During a resistance-welding operation, a workpiece is pressed between two electrodes and an electrical current is passed between the electrodes. Based on the Joule's law, the resistance in the electrode-worksheet and worksheet-worksheet interfaces generates the heat that locally melts and binds the sheets together. The section, where the two pieces of metal melt and then cool down to form one piece is called a nugget. In fact, the nugget is the area that actually joins the two pieces of metal together. The quality and strength of spot welds in a structure determine the performance quality of that structure, depending thoroughly on the nugget size. The nugget size should be larger than a certain volume to secure the strength of a welded joint. On the other hand, changing the parameters to obtain a very large nugget size leads to an explosion in the weld zone which reduces the strength of a welded joint. The nugget size is usually between 4 and 8.5 mm, completely depending on

the sheet thickness. So, a control of the welding parameters is necessary to obtain a high weld quality and to increase a vehicle's life.

Although there are many researches being carried out on the effects of welding parameters on the nugget size in a spot weld of steels and many approaches being developed and recommended for a nugget-size prediction, the studies on aluminum-alloy spot welds are scarce. Darwish et al.[4–6] completed many studies on the spot welds of commercial B. S. 1050 aluminum alloys. Khan et al.[7] and Fangjie et al.[8] used a finite-element model (FEM) to predict the nugget size for a spot weld of an aluminum alloy. Sun et al.[9] studied the failure load and the failure mode of spot welds of aluminum alloys 5182-O and 6114-T4 with a cross-tension test. Pereira et al.[1] carried out studies on the effect of process parameters on the strength of spot welds in 6082-T6 aluminum alloys with a sheet thickness 1 mm under a quasi-static tensile test and recommended a model for calculating the critical nugget size to achieve the PL failure mode. Recently, Han et al.[10] have studied the failure load in lap shear, cross tension and coach peel of resistance-spot-welded aluminum AA5754.

The use of a finite-element analysis (FEA) decreases the main costs associated with the nugget-size measurement tests; however, due to a high complexity of a spot weld, its FEA models are very time-consuming, requiring high-speed computers. The method of artificial neural networks (ANNs) is considered as an effective approach for solving non-linear problems. A quick learning ability and high-speed solutions of ANNs have led to a more extensive use of this method.[11] In recent years, the use of ANNs in modelling resistance spot welds has attracted the attention of researchers. Park[12] and Martin[13] employed these networks to predict the fatigue life and improvement in the quality of spot welds. Also, Cortez[14] used an ANN to investigate the weldability of different metals with the spot-weld process.

The joint use of an FEA and ANN can eliminate the high costs of laboratory tests and significantly shorten
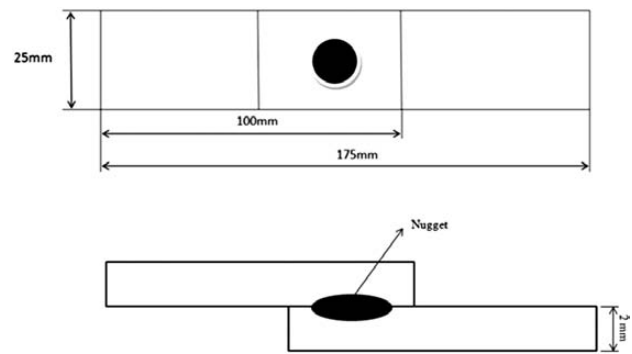

Figure 1: Dimensions of the samples (dimensions in millimeters, not to scale)
Slika 1: Dimenzije vzorcev (dimenzije v milimetrih, ni v merilu)

the time needed for a solution. This idea has been the basis of our study. In this study, a FEA model along with an ANN has been adopted to predict the nugget size for the spot welds of a thick aluminum 6061-T6 sheet 2 mm. At first, the experimental procedures utilized to prepare the spot-welded samples and the nugget-size measurement are shown. Then, the basics of the axi-symmetrically coupled, thermal-electrical-mechanical FEA are presented. The structure of an ANN model is provided in Section 4. The results are discussed in Section 5 and the conclusions are given in last section.

2 EXPERIMENTAL PROCEDURES

The thick, heat-treatable aluminum-alloy 6061-T6 sheets 2 mm were welded as a lap joint with the dimensions of 100 mm × 25 mm × 2 mm (**Figure 1**). The nominal chemical composition and mechanical properties of the base material are given in **Table 1**. Before spot welding, each sheet was cleaned mechanically with sandpaper and the welding process was performed with a NIMAK type PMP11 DGS, AC power machine with the nominal welding power of 200 kV A and copper electrodes. Nine different series of welding parameters were

Table 1: Mechanical properties and chemical composition of aluminum alloy 6061-T6 (mass fractions, w/%)
Tabela 1: Mehanske lastnosti in kemijska sestava zlitine aluminija 6061-T6 (masni deleži, w/%)

Yield strength	Tensile strength	Hardness	Al	Si	Mn	Mg	Fe	Cu	Cr
MPa	MPa	Vickers	%	%	%	%	%	%	%
276.0	310.0	107.0	97.0	0.6	0.1	1.0	0.5	0.2	0.1

Table 2: Resistance-spot-welding operations for aluminum 6061-T6
Tabela 2: Parametri točkastega varjenja aluminija 6061-T6

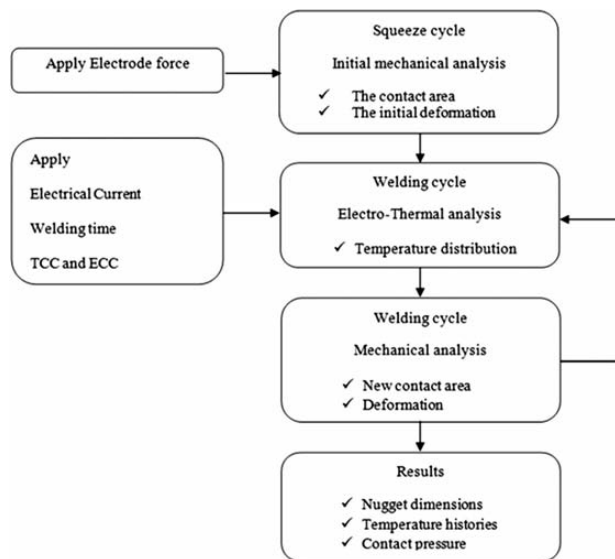| Sample No.	Electrical current	Welding time	Electrode force	Sample No.	Electrical current	Welding time	Electrode force
	(kA)	(cycles)	(N)		(kA)	(cycles)	(N)
1	36	4	4033	6	37	4	4033
2	36	5	4033	7	38	4	4033
3	36	6	4033	8	39	4	4033
4	36	7	4033	9	40	4	4033
5	36	8	4033	–	–	–	–

used for the welding of 27 samples (3 samples for each series of parameters). The welding conditions were based on the recommendations by AWS[15] in order to achieve the minimum nugget size and avoid an expulsion in welding.

Table 2 summarizes these 9 series with the corresponding welding parameters. As seen in **Table 2**, very small expulsions occurred in welding Samples 5 and 9. To measure the nugget size, the samples were first cut along the center line and then mounted, polished and etched. The nugget-size measurements were done using an interaction of an optic microscope and special software developed for image processing.

3 FINITE-ELEMENT ANALYSIS

Different phenomena (e.g., mechanical, thermal, electrical, metallurgical, etc.) are involved in resistance-spot-welding operations. Due to a complexity of the spot-welding process and the extensive connections between these different fields, a simulation of these operations is very difficult. In this study, an axi-symmetrically coupled, thermal-electrical-mechanical FE model was used for simulating a spot weld. To create the FE model for the simulation of spot welding of aluminum 6061-T6, the commercial ANSYS12.1 software and the APDL environment were used. To achieve high accuracy, the temperature-dependent properties were defined for the material.

The solving algorithm of the finite-element model is illustrated in **Figure 2**. The first step of the welding process is the squeeze cycle. In this step, only the electrode force is applied to the model and the structural elements are used for the initial mechanical analysis to determine the initial deformation and the contact-area shape. In the welding cycle, the electrical current is
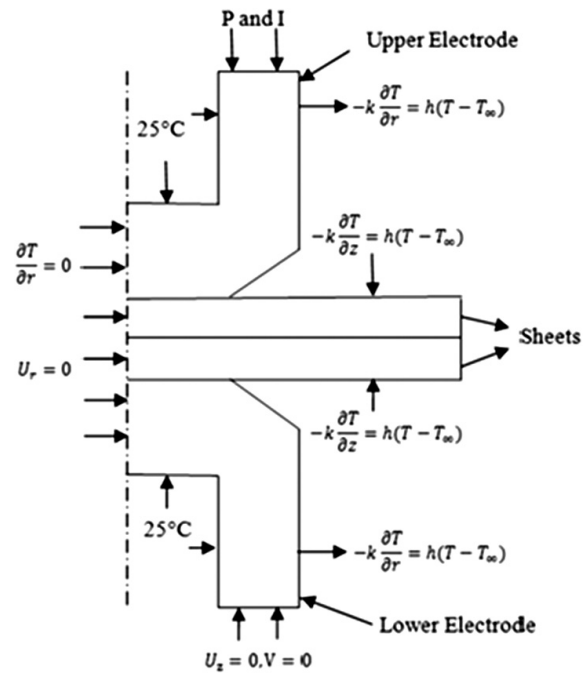
applied to the top surface of the upper electrode and by using the thermal-electrical elements the heat generation is calculated for each increment from the fully coupled model.

All the mechanical, electrical and thermal boundary conditions used in the FE model are presented in **Figure 3**. In the welding cycle, the *rms* electrical current is applied uniformly to the top surface of the upper electrode and after passing through the electrode-sheet and sheet-sheet contact areas, it reaches the bottom surface of the lower electrode, where zero electrical voltage has been applied. For all the process cycles, a constant water temperature of 25 °C was considered for the electrode's water channel. Since an exact estimation of the convection-heat-transfer coefficient for the surfaces of the sheets and electrodes that are in contact with air is very difficult as it depends on numerous factors such as the air-flow velocity and surface quality, for all the surfaces that are in contact with air, the convection-heat-transfer coefficient was determined to be constant and equal to 12 W m^{-2} K^{-1}.[16] The ambient room temperature was assumed as 20 °C. The electrode force, as a uniform compressive load, was applied to the upper electrode, as shown in **Figure 3**.

All the equations in this work are based on a two-dimensional cylindrical coordinate system. Equation 1 presents the governing equation for calculating the electrical potential φ for the whole model:

$$\frac{\partial}{\partial r}\left(C_0 \frac{\partial \varphi}{\partial r}\right) + \frac{C_0}{r}\frac{\partial \varphi}{\partial t} + \frac{\partial}{\partial z}\left(C_0 \frac{\partial \varphi}{\partial z}\right) = 0 \qquad (1)$$

Figure 2: Flowchart of the finite-element solving algorithm
Slika 2: Shema reševanja algoritma s končnimi elementi

Figure 3: Axi-symmetric finite-element model used for a spot-weld simulation with boundary conditions
Slika 3: Osnosimetrični model končnih elementov, uporabljen za simulacijo točkastega zvara, z robnimi pogoji

where r is the radial distance, z is the distance in the axis direction and C^s is the electrical conductivity. Based on the Joule heat equation, the heat generation per unit volume, q, can be shown with equation 2:

$$q = \frac{\varphi^2 t}{R} \qquad (2)$$

where t is the time and R is the material electrical resistance. The governing equation for the transient-temperature-field distribution considering the electrical-resistance heat can be presented with equation 3:

$$\rho t \frac{\partial T}{\partial t} = \frac{\partial}{\partial r}\left(k\frac{\partial T}{\partial r}\right) + \frac{k}{r}\frac{\partial T}{\partial r} + \frac{\partial}{\partial z}\left(k\frac{\partial T}{\partial r}\right) + \dot{q} \qquad (3)$$

where ρ is the material density, C is the heat capacity, T is the temperature, $\dot{q}$ is the rate of heat generation per unit volume and k is the thermal conductivity. For a stress and strain analysis, the governing equation is described in an incremental form for the finite-element model:

$$\{\Delta\sigma\} = [D]\ \{\Delta\varepsilon\} + \{C\}\Delta T \qquad (4)$$

where vectors $\{\Delta\sigma\}$ and $\{\Delta\varepsilon\}$ are stress and strain increments, respectively, matrix $[D]$ is the elastic-plastic matrix and vector $\{C\}$ can be defined as:

$$\{C\} = -[D^0]\left(\{\alpha\} + \frac{\partial[D^0]^{-1}}{\partial T}\right) \qquad (5)$$

Here matrix $[D]$ is the elastic matrix and matrix $\{\alpha\}$ is the coefficient of thermal expansion.

4 ARTIFICIAL NEURAL NETWORK

A back-propagation ANN was employed to predict the nugget size for a spot weld. Structurally, every ANN is made up of three sections (**Figure 4**). The initial section corresponds to the input layer of an ANN. In the present study, the two main parameters, the welding current and the welding time, were used as the network inputs. The number of layers and neurons of the middle section, or the hidden layer, are determined with the trial-and-error metho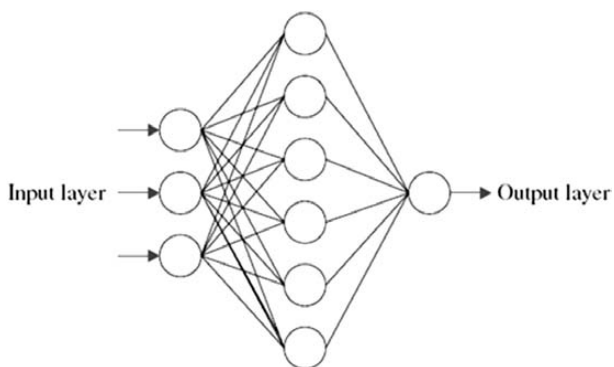d. The end section of the network is the output layer. In this study, the nugget diameter was used as the ANN output due to its significant role in the quality of the welded joint.

The training algorithm of Levenberg-Marquad was employed to train the ANN. This training algorithm has a very quick learning speed. The performance index used in the training was the mean squared error (*MSE*) defined as:

$$MSE = \frac{1}{N}\sum_{i=1}^{N}(r_i - \hat{r}_i)^2 \qquad (6)$$

where r_i is the actual variable, while $\hat{r}_i$ is the estimated variable and N is the number of data samples. In the present study, the tolerance for *MSE* was selected as 0.0001.

5 RESULTS AND DISCUSSIONS

Since the weld quality and strength are completely related to the nugget size, the metallographic analysis and microstructure studies are employed to better understand the microstructures of the weld zones and to correctly specify and measure the nugget diameter. **Figure 5** shows a typical macrostructure of a spot-welded sample. Three distinct zones are clearly observed: the base metal (BM), the heat-affected zone (HAZ) and the fusion zone (FZ) or the nugget. The microstructure investigation shows two different zones in the nugget area: the grains with columnar structure oriented in the direction of the heat flow around the nugget and a new nucleation zone in the center, as seen in **Figure 6**. The reason for the two different microstructures in the nugget zone could be a variation in the cooling rate within the nugget zone.[1]

The microstructure of the HAZ is different from that of the nugget. In the area between the nugget and HAZ, there is a thin zone with large and coarse grains; it could be attributed to an abnormal grain growth due to an extremely high temperature. However, beyond this zone, the HAZ consists of very small and fine grains, as seen in **Figure 6**.
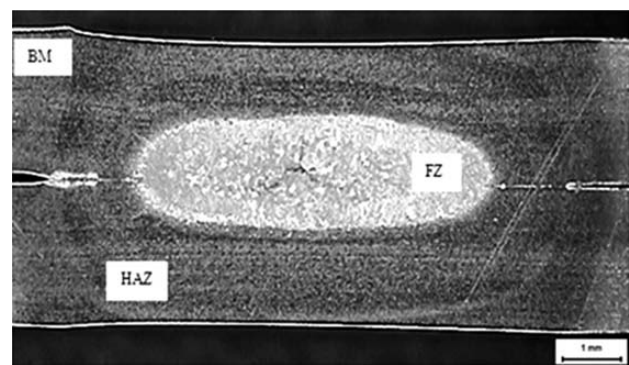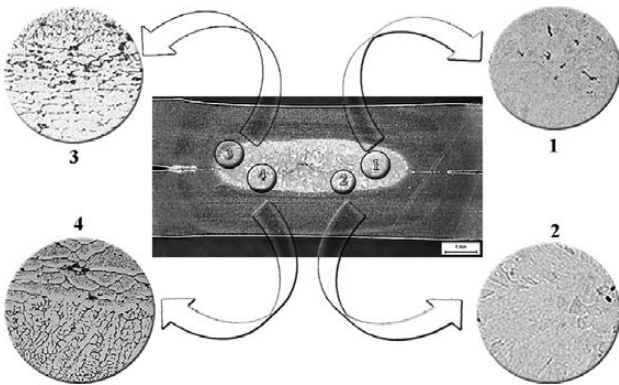

Figure 4: Typical artificial neural network
Slika 4: Značilna umetna nevronska mreža

Figure 5: Different zones in the weld area, FZ: nugget zone, HAZ: heat-affected zone and BM: base material
**Slika 5:** Različna področja v zvaru, FZ: področje pretalitve, HAZ: toplotno vplivano področje in BM: osnovni material

Figure 6: Microstructure of the nugget (Sample 5)
**Slika 6:** Mikrostruktura v območju pretalitve (vzorec 5)
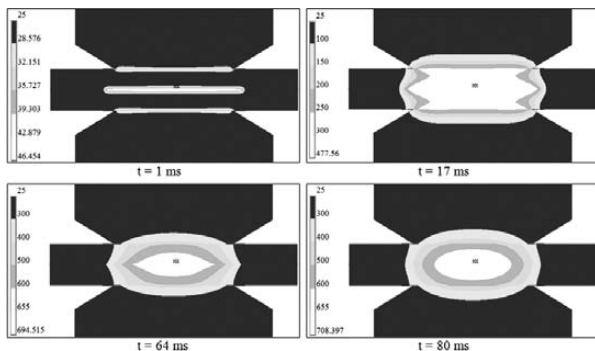
Figure 7: Nugget development in the finite-element model (welding current: 36 kA, electrode force: 4033 N), welding time: a) 1 ms, b) 17 ms, c) 64 ms and d) 80 ms
Slika 7: Rast področja pretalitve pri modelu končnih elementov (varilni tok: 36 kA, pritisk elektrode: 4033 N), čas varjenja: a) 1 ms, b) 17 ms, c) 64 ms in d) 80 ms
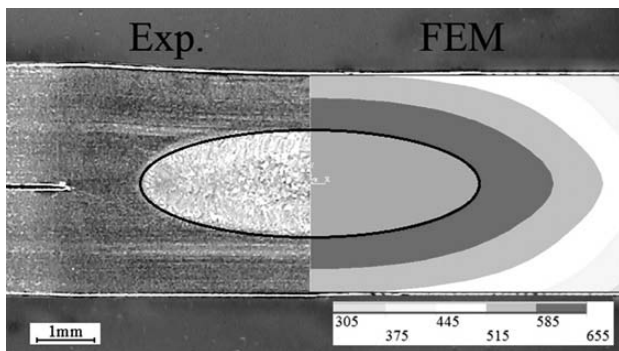
Figure 8: Comparison between the simulated nugget obtained with the FEM and the actual nugget of Sample 1
Slika 8: Primerjava med simuliranim področjem pretalitve s FEM in resnično velikostjo področja pretalitve pri vzorcu 1

Figure 7 illustrates the steps of the nugget formation in the FE model. To validate the FE model results, the model was compared with the data obtained with the nugget-size measurements. In **Figure 8**, the FEM nugget size is compared with the actual nugget size for Sample 1. **Figure 9** compares the results of the FEM and the experimental tests for all the samples presented in **Table**
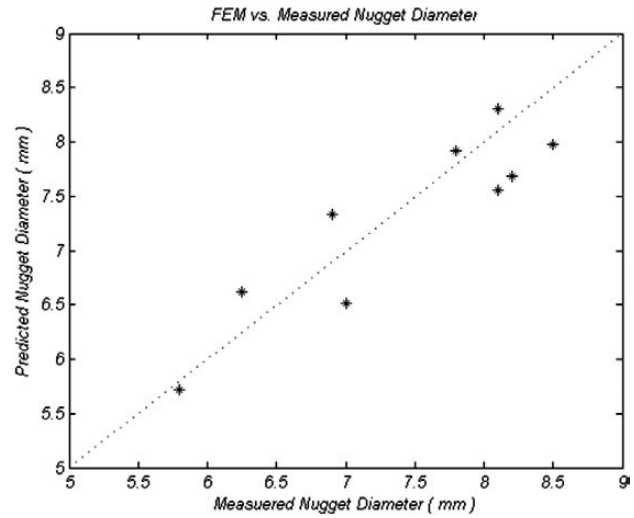
Figure 9: Comparison between the nugget diameter obtained with the FEM and the data obtained with the experimental test presented in **Table 2**
Slika 9: Primerjava med premerom pretaljenega področja, dobljenega s FEM in eksperimentalnimi podatki, prikazanimi v **tabeli 2**

1. The FEM results indicate that the presented model has a good accuracy.

As mentioned before, the welding conditions were based on the recommendations by AWS[15] in order to achieve the minimum nugget size (5.6 mm for the sheets with a thickness 2 mm) and avoid an expulsion in the welding. Considering the results obtained from a previous study,[17] for thick aluminum 6061-T6 sheets 2 mm, with a weld-nugget diameter of above 8.5 mm, the spattering of melt during a spot-welding operation is predictable. Therefore, the selection of the spot-welding parameters is based on the simulation results of the FE analysis with the aim to achieve a weld-nugget diameter between 5.6 mm and 8.5 mm. **Table 3** shows the selected spot-welding parameters obtained from the FEA for the nugget-size prediction with the ANN. Of the 54 sets of parameters presented in **Table 3**, five samples were randomly selected and used for testing the ANN, and the remaining samples (49 samples) were used for training the ANN.

Table 3: Considered spot-weld parameters for the ANN creation
Tabela 3: Parametri točkastega zvara, upoštevani pri postavitvi ANN

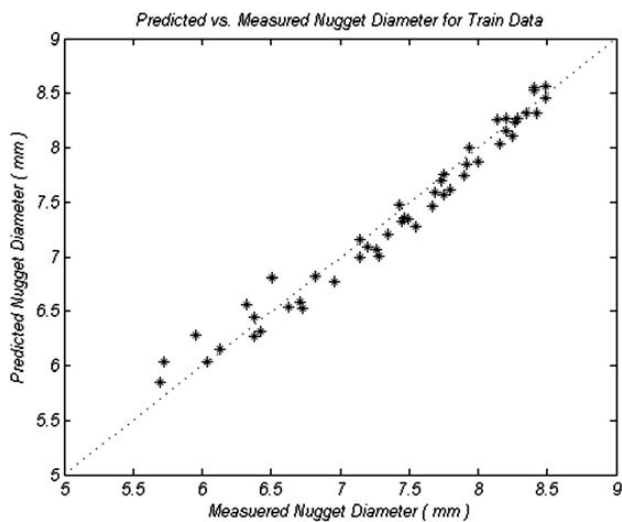| Electrode force (N)	Welding time (Cycles)	Welding current (kA)
4033	4, 4.5, 5, 5.5, 6, 6.5, 7 and 7.5	36
4033	4, 4.5, 5, 5.5, 6, 6.5, 7 and 7.5	36.5
4033	3.5, 4, 4.5, 5, 5.5, 6, 6.5 and 7	37
4033	3.5, 4, 4.5, 5, 5.5, 6 and 6.5	37.5
4033	3.5, 4, 4.5, 5 and 5.5	38
4033	3.5, 4, 4.5, 5 and 5.5	38.5
4033	3, 3.5, 4, 4.5 and 5	39
4033	3, 3.5, 4 and 4.5	39.5
4033	3, 3.5, 4 and 4.5	40

Figure 10: Results of the neural-network training
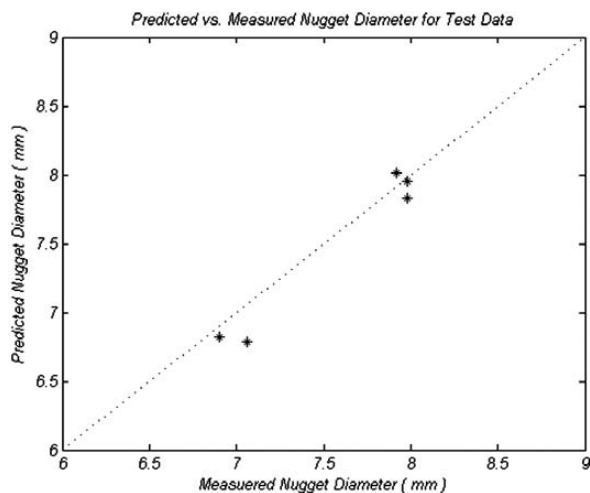**Slika 10:** Rezultati, dobljeni z usposabljanjem nevronske mreže

Figure 11: Results of the neural-network test
Slika 11: Rezultati preizkusa nevronske mreže

By testing different structures of the ANN, it was determined that an ANN with one hidden layer and eight neurons in this layer has the lowest error in the prediction of the nugget diameter. **Figure 10** shows the results of training a developed ANN on the basis of the data obtained from the FE analysis. As this figure indicates, the presented ANN was well trained.

After training the created ANN, the network was tested by employing the five samples that had not been used in the training. The result of the testing is shown in **Figure 11**. The obtained results demonstrate that the created ANN has a good accuracy (less than 3 % of the absolute average error) in the prediction of the nugget diameter, based on the listed spot-welding parameters. So, this network can be used reliably for predicting the nugget diameter in the spot weld of thick aluminum 6061-T6 sheets 2 mm.

6 CONCLUSIONS

In this study, the nugget size for the spot weld of an aluminum 6061-T6 sheet with a thickness of 2 mm was predicted with a combination of a finite-element analysis and artificial neural network. The findings obtained from the nugget-size measurements, the FEA and the ANN can be summarized as follows:

- The comparison between the FEA results and the measured nugget size indicates that the presented model has a good accuracy in the prediction of the nugget size and that, by using this model, the nugget size for spot welds can be rapidly investigated.
- The ANN model created using the results of the FEA has a very good accuracy (less than 3 %) in the prediction of the nugget size, based on the spot-welding parameters of the welding current and the welding time.
- After a verification of FEA and ANN results, through the use of the FEA and ANN, the size of the nugget in a spot weld can be well predicted, reducing the number of the nugget-size measurements.

7 REFERENCES

[1] A. M. Pereira, J. M. Ferreira, A. J. Loureiro, D. M. Costa, P. J. Bartolo, Material and Design, 31 (**2010**), 2454–2463
[2] Y. J. Chao, Journal of Engineering Materials and Technology, 125 (**2003**), 125–132
[3] X. Sun, E. V. Stephens, M. A. Khaleel, Engineering Failure Analysis, 15 (**2008**), 356–367
[4] S. M. Darwish, S. D. Al-Dekhial, Journal of Materials Processing Technology, 91 (**1999**), 43–51
[5] S. M. Darwish, S. D. Al-Dekhial, International Journal of Machine Tools & Manufacture, 39 (**1999**), 1589–1610
[6] S. M. Darwish, International Journal of Adhesion & Adhesives, 23 (**2003**), 169–176
[7] J. A. Khan, L. Xu, Y. Chao, K. Broach, Numerical Heat Transfer Part A, 37 (**2000**), 425–446
[8] C. Fangjie, J. Zhang, S. Hu, P. Shan, Trans. Tianjin. University, 17 (**2011**), 28–32
[9] X. Sun, E. V. Davies, R. W. Khaleel, D. J. Spinella, Welding Journal, 83 (**2004**), 308–318
[10] L. Han, M. Thornton, D. Boomer, M. Shergold, Journal of Material Processing Technology, 211 (**2011**), 513–521
[11] M. S. Choobi, M. Haghpanahi, M. Sedighi, Computational Materials Science, 62 (**2012**), 152–159
[12] J. M. Park, H. T. Kang, Material and Design, 28 (**2008**), 311–325
[13] O. Martin, M. Lopez, F. Martin, Journal of Materials Processing Technology, 183 (**2007**), 226–233
[14] V. H. L. Cortez, F. A. R. Valdes, L. T. Trevino, Materials & Manufacturing Processing, 24 (**2009**), 1412–1417
[15] American welding society, Recommended practices for resistance welding, AWS C1.1M/C1.1:2000, AWS, New York, 2003
[16] X. Long, S. K. Khanna, Science and Technology of Welding and Joining, 10 (**2005**), 88–94
[17] D. Afshari, M. Sedighi, Z. Barsoum, R. L. Peng, Journal of Engineering Manufacture Part B, 226 (**2012**), 1026–1032